

Microwave dielectric study of spin-Peierls and charge-ordering transitions in (TMTTF)₂PF₆ salts

Alexandre Langlois, Mario Poirier, and Claude Bourbonnais

Regroupement Québécois sur les Matériaux de Pointe, Département de Physique, Université de Sherbrooke, Sherbrooke, Québec, Canada J1K 2R1

Pascale Foury-Leylekian, Alec Moradpour, and Jean-Paul Pouget

Laboratoire de Physique des Solides, CNRS UMR 8502, Université Paris-Sud, 91405 Orsay Cédex, France

(Received 23 July 2009; revised manuscript received 3 February 2010; published 3 March 2010)

We report a study of the 16.5 GHz dielectric function of hydrogenated and deuterated organic salts (TMTTF)₂PF₆. The temperature behavior of the dielectric function is consistent with short-range polar order whose relaxation time decreases rapidly below the charge-ordering temperature. If this transition has more a relaxor character in the hydrogenated salt, charge ordering is strengthened in the deuterated one where the transition temperature has increased by more than thirty percent. We give the first account of anomalies in the dielectric function related to the spin-Peierls ground state revealing some interaction between both phases in their domain of coexistence in temperature. The variation of the spin-Peierls ordering temperature obtained under magnetic field completes the structure of the phase diagram at low field and are analyzed in the framework of the mean-field prediction.

DOI: [10.1103/PhysRevB.81.125101](https://doi.org/10.1103/PhysRevB.81.125101)

PACS number(s): 71.20.Rv, 71.30.+h, 77.22.Ej

I. INTRODUCTION

The Fabre [(TMTTF)₂X] and Bechgaard [(TMTTF)₂X] series of charge transfer salts show a very rich sequence of competing ground states when either hydrostatic or chemical pressure is applied.¹ In the universal phase diagram of these series, the (TMTTF)₂X are Mott insulators that develop a charge ordered (CO) state.^{2,3} This state is followed at lower temperature by either an antiferromagnetic Néel or a lattice distorted spin-Peierls (SP) phase. This pattern turns out to be affected by pressure, anion X substitution, and to some degree by the deuteration of the methyl groups. This is how the (TMTTF)₂X can be moved along the pressure axis with respect to the (TMTSF)₂X series for which metallic, antiferromagnetic, and superconducting phases can be stabilized. In low pressure conditions, the (TMTTF)₂X salts thus appear as model correlated quasi-one-dimensional systems to study the interplay between spin, charge, and lattice degrees of freedom.

In several (TMTTF)₂X salts with octahedral anions X, the CO transition follows and in some cases coincides with the 4k_F charge localization.^{4–8} The first evidences of this transition in X=SbF₆ and AsF₆ came from transport measurements.^{4,5,9} The transition was dubbed “structureless,” because of the absence of any structural modification associated to it.⁹ The CO character of the transition only comes much later from the low frequency dielectric response,^{6,10} and NMR experiments in which charge disproportionation in the unit cell was unveiled.^{7,11,12} The CO character of the transition is also found from infrared spectroscopy measurements.¹³ The CO transition is also accompanied by the onset of a ferroelectric state revealed by the divergence of the low frequency dielectric constant.¹⁴

As regards to spin degrees of freedom, these are essentially decoupled from the progressive charge localization or the CO transition. However, in compounds like X=PF₆ in normal pressure conditions, a SP transition takes place at T_{SP} ≈ 18 K (hydrogenated)^{15,16} and 13 K (deuterated).¹⁷ The

spin singlet state that goes with the SP lattice distortion has been borne out by spin susceptibility,^{18–20} and NMR spin relaxation rate,^{18,21,22} whereas a sizable part of the magnetic field-temperature phase diagram for the PF₆ salt has been obtained by high-field NMR and magnetization studies.²³ In the PF₆ salt, the observation of x-ray 2k_F diffuse scattering indicates the presence of lattice precursors of the SP transition below 60 K (Ref. 15); these open a spin pseudo gap,²⁴ as exhibited by magnetic susceptibility and NMR data.^{18,20,25}

Finally, lattice expansion effects were recently observed at both CO and SP transitions of the PF₆ and AsF₆ salts.^{26,27} Indeed, distinct lattice effects were found at T_{CO} in the uniaxial expansivity along the interstack c* direction, signaling an active role of anion X lattice degrees of freedom in the stabilization of the CO ground state, and further clarifying the ferroelectric nature of the transition. It is also the c*-axis expansivity that is the most strongly affected at the SP transition.

In this paper, we address the issue of interplay between charge, spin and lattice degrees of freedom by studying the 16.5 GHz complex microwave dielectric function of (TMTTF)₂PF₆ single crystals under magnetic field. The dielectric anomalies are shown to take place at both the CO and SP transitions. We report the first evidence of an interaction between both ground states in (TMTTF)₂PF₆. The increase of T_{CO} and the drop of T_{SP} are also confirmed for the deuterated compound as a negative shift on the pressure scale. The phase diagram of (TMTTF)₂PF₆ at low magnetic field is clarified in the SP sector. Up to 18 T, T_{SP} is found to vary quadratically with field and the results are compared to the mean-field prediction obtained by Cross.²⁸ Other magnetic fields effects on the polarizability of the system are found and ascribed to the interaction between CO and SP orderings. Finally, we report the existence of thermal relaxation effects in the deuterated compound near the SP transition.

II. EXPERIMENT

Hydrogenated (H_{12}) $(TMTTF)_2PF_6$ single crystals were grown from THF using the standard constant-current (low current density) electrochemical procedure. The synthesis of the fully deuterated $TMTTF-d_{12}$ (D_{12}) was attempted using the procedure of Wudl *et al.*²⁹ for the preparation of 3-chloro-2-butanone- d_7 . However, this awkward very poorly described procedure led in our hands to traces, if any, of the desired chloroketone. Therefore, we worked out a more practical and shortened procedure to prepare this compound: perdeuterioacetoin was first prepared from perdeuteriobiacyetyl³⁰ according to the literature³¹ and the procedure for the conversion of allylic alcohols into chlorides³² applied to this -hydroxy ketone. To the cooled mixture of the latter with a slight excess of PPh_3 in sulfolane was added dropwise a solution of hexachloroacetone in sulfolane, and the reaction mixture stirred at room temperature for two weeks; a flash distillation of the reaction mixture and a subsequent distillation at atmospheric pressure led to the desired chloroketone with a (up to) 50% yield. Starting from this deuterated chloroketone, $TMTTF-d_{12}$ was obtained using usual procedures and the corresponding deuterium incorporation-levels estimated by NMR to be 97.5 %.

The crystals have the shape of a needle oriented along the chain axis a , from which were cut short slabs of typical dimensions $2.4 \times 0.8 \times 0.4$ mm³ for H_{12} and $1.5 \times 0.4 \times 0.07$ mm³ for D_{12} . We used a standard microwave cavity perturbation technique³³ to measure the complex dielectric function $\epsilon^* = \epsilon' + i\epsilon''$ along the a axis. A copper cavity resonating in the TE_{102} mode was used at 16.5 GHz. The organic slab is inserted in a mylar envelope and immobilized by thin cotton threads to prevent any stress or movement during thermal cycling. The envelope is glued on a quartz rod to allow its insertion in the cavity and the precise orientation of the slab along the microwave electric field. Following the insertion of the sample, changes in the relative complex resonance frequency $\Delta f/f + i\Delta(1/2Q)$ (Q is the cavity quality factor) as a function of temperature are treated according to the depolarization regime analysis after subtraction of the envelope contribution. With this microwave technique, the slab's length is chosen to adjust the relative frequency shift under one percent (a few tenths for the maximum value) while keeping the length/width ratio high enough to use the approximation of a prolate ellipsoid. For each compound, we tested slabs with slightly different geometries (different lengths) and we always obtained the same temperature dependences for the dielectric function ϵ^* ; because of the ellipsoid approximation, absolute values can only be measured within 30% of accuracy. A magnetic field up to 18 T could be applied along the c^* axis.

III. RESULTS AND DISCUSSION

When the temperature is decreased from 300 K, the dielectric function of both H_{12} and D_{12} salts shows a similar behavior: the real part ϵ' decreases smoothly with a faster rate below 100 K before its saturation at low temperatures; the imaginary part ϵ'' rather increases first, reaches a maximum below 100 K and decreases rapidly toward zero at low

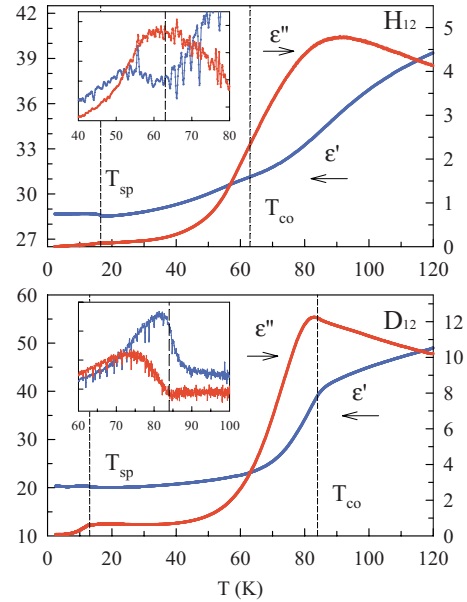


FIG. 1. (Color online) Temperature dependence of the dielectric function along the chain axis at 16.5 GHz: top panel PF_6 (H_{12}), lower panel PF_6 (D_{12}); definition of T_{CO} from the derivatives shown in the insets.

T . These temperature dependences reproduced on a few samples are likely associated to the CO transition. An example of typical temperature profiles are presented below 120 K in Fig. 1. The CO transition in the H_{12} salt is known to be of the relaxor type and the data shown in Fig. 1, which extend the low frequency dielectric measurements,^{6,10} are fully consistent with this picture. With such a type of transition, the determination of an ordering temperature T_{CO} appears to be complicated. Following the argument that a criterion common to both parts of the complex dielectric function must be used to determine the CO transition temperature, we deduced $T_{CO} \approx 63$ K by observing only one common feature on the temperature derivative (see inset of Fig. 1, top panel), a value in full agreement with previous works.⁷ For the D_{12} salt, the features below 100 K are found to be much sharper, an observation which is consistent with a stabilization of the CO transition upon deuteration. If we apply the same criterion used for the H_{12} salt (temperature derivative shown in the lower panel inset), we obtain $T_{CO} = 84$ K, a value identical to the one deduced from ESR measurements.³⁴ Because of its high sensitivity to small dielectric changes, our single frequency microwave technique show clear (although small) anomalies in the low temperature range at T_{SP} . Such small anomalies, that could not be observed in previous low frequency dielectric measurements on the H_{12} compound,¹⁰ will be analyzed later.

Earlier analysis of the dielectric response measurements performed at lower frequencies (10^3 – 10^7 Hz),^{10,14} showed that the $\epsilon'(T)$ data can be qualitatively understood by assuming the existence of critical slowing down near a phase transition. The maximum of $\epsilon''(T)$ was used to obtain an effective temperature dependent relaxation time $\tau(T)$. In a similar way, we propose to model the frequency dependence of the dielectric function by using a monodispersive Debye relax-

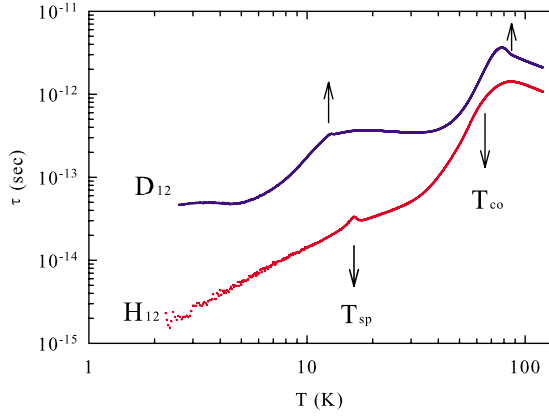


FIG. 2. (Color online) Temperature dependence of the relaxation time $\tau(T)$ obtained from Eq. (1).

ation term to get the temperature dependence of the relaxation time at a single frequency ω from the ratio

$$\tau(T) = \frac{\epsilon''(T)}{\omega[\epsilon'(T) - \epsilon_\infty]}. \quad (1)$$

The temperature profile $\tau(T)$ deduced from Eq. (1) is not very sensitive to the exact value chosen for the high frequency dielectric constant ϵ_∞ , which was fixed to 2.5.³⁵ The $\tau(T)$ curves deduced for both salts are shown in Fig. 2 on a log-log scale. These relaxation time curves are quite different from the data collected at lower frequencies:¹⁰ not only are the absolute values smaller by four orders of magnitude at 100 K, but the temperature variation is the opposite below the CO transition. Indeed, for the H_{12} salt, although $\tau(T)$ increases below 120 K, it presents a maximum around 80 K and decreases rapidly by more than one order of magnitude down to 40 K. Below, $\tau(T)$ keeps decreasing, but with a different slope. Between 80 K and the lowest temperature reached at 2 K, $\tau(T)$, has practically decreased by three orders of magnitude, while the low frequency data rather show an increase in the same size with only a change of slope near T_{CO} .¹⁰ A kink is observed at T_{SP} followed by a small variation of the decreasing rate. If one looks at the relaxation time for the D_{12} salt in Fig. 2, it shows a similar behavior from 120 to 40 K, but the maximum in $\tau(T)$, which is sharper, occurs just below T_{CO} . For $T < 40$ K, the decrease is less pronounced than for the H_{12} salt due to an additional contribution to the dielectric function, and which will be discussed in more detail below.

The discrepancy between microwave and low frequency data for the H_{12} salt may be linked to the nature of the relaxor ferroelectric state and to the four orders of magnitude difference in frequency. The microwave experiment is likely to be sensitive to the spatial variation in polar order taking place at relatively short length scale, which is characterized by a short relaxation time. As we move further below T_{CO} on the temperature axis, these polar fluctuations decrease in size yielding a decrease of the dielectric constant and of the corresponding losses, as depicted in Figs. 1 and 3.

As regards to the increase in T_{CO} by deuteration, it has been shown recently that the collective displacement of

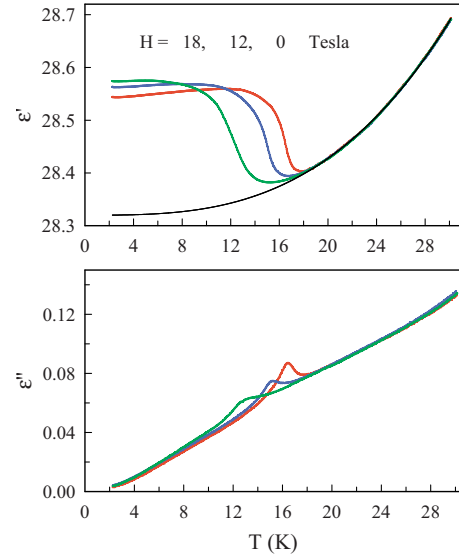


FIG. 3. (Color online) Temperature dependence of the dielectric function near T_{SP} for the H_{12} salt in 0 (red), 12 (blue) and 18 (green) Tesla. The black line is the $a+bT^3$ fit.

counteranions X^- is directly coupled to the charge modulation along the stacks²⁶ and that the stabilizing potential grows not only with the size of the anion but also upon deuteration.¹⁷ The increase in T_{CO} revealed by the microwave experiment on a deuterated crystal is consistent with this picture.

Let us examine now the anomalies appearing in the SP state. We show in Fig. 3 the dielectric function of the H_{12} salt below 30 K. In zero magnetic field, the real part ϵ' increases abruptly below 16.5 ± 0.1 K and then decreases slightly as we move sufficiently down in temperature. To the increase in ϵ' corresponds a peak in the imaginary part ϵ'' . The latter decreases to zero with a larger slope. These anomalies are consistent with the onset of the SP long-range order at $T_{SP} \approx 16.5$ K.¹⁷ This is also compatible with the application of a magnetic field, which depresses T_{SP} down to $12.5 \text{ K} \pm 0.2$ at 18 T. Except for a small temperature interval where critical SP fluctuations enhance the dielectric constant, the magnetic field has no noticeable effect above T_{SP} , where ϵ' follows a perfect T^3 power law up to 30 K, as indicated by the black line extrapolated toward the very low temperature domain (top panel). The microwave absorption is very low in this temperature range and this yields larger imprecisions on $\epsilon''(T)$ when the field is applied. Nevertheless, we found a T^x power law with x lying in the 1.4–1.6 interval for $T > T_{SP}$. We have subtracted these power laws extrapolated to zero to obtain the contribution of the SP state to the dielectric function at low temperatures, $\Delta\epsilon'$ and $\Delta\epsilon''$, shown in Fig. 4.

The anomaly shown by $\Delta\epsilon'$ as we dip into the SP ordered region reveals an increase of polarizability in the presence of the lattice distortion. This is compatible with a reduction of the amplitude of the CO order parameter as the SP order sets in, an effect also consistent with previous NMR and optical measurements on the cousin SP compound $(TMTTF)_2AsF_6$.^{12,13} It is worth noting that the amplitude of the variation shown by $\Delta\epsilon'$, as a result of SP ordering, is at the most 1% of the background value exhibited in Fig. 3.

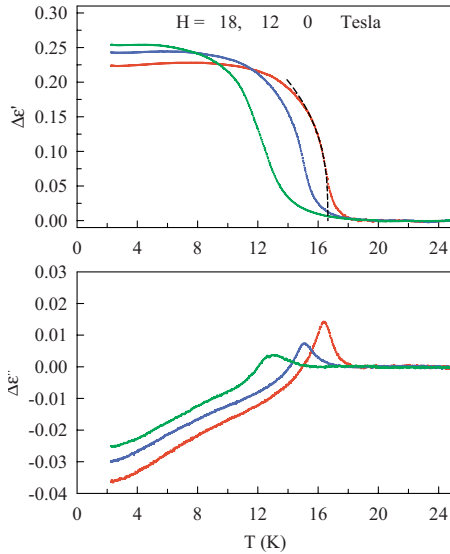


FIG. 4. (Color online) Contribution of the SP state to the dielectric function as a function of temperature in 0, 12, and 18 T field. The dashed line is a fit to $\Delta\epsilon' \propto (T_{SP} - T)^\beta$ ($\beta \approx 0.36$) in the critical region of the SP transition.

While the anomaly indicates that the lattice distortion does alter the charge ordered state of $(\text{TMTTF})_2\text{PF}_6$, the relative smallness of the effect may explain the difficulty for charge sensitive probes to detect any reduction in CO ordering by the SP state in this material.¹³

The rapid increase in the dielectric response below T_{SP} suggests a temperature dependence of $\Delta\epsilon'$ governed by the criticality of the SP order parameter. A log-log plot analysis of the $\Delta\epsilon'$ data reveals indeed that the critical behavior can be reasonably fitted with a power law $\Delta\epsilon' \propto (T_{SP} - T)^\beta$. Using the value T_{SP} obtained from the maximum slope of $\Delta\epsilon'$, the exponent $\beta \approx 0.36$ is extracted (dashed line of Fig. 4). This non-mean-field value is consistent with the β expected for a SP—one-component—order parameter in three dimensions.

Considering now the magnetic field dependence, T_{SP} is found to be progressively depressed under field. The transition's width increases due to a larger temperature interval of SP critical fluctuations. However, at variance with other spin-Peierls systems such as CuGeO_3 ,³⁶ or Peierls systems,³⁷ for which the order parameter is independent of magnetic field in the low temperature limit,³⁸ $\Delta\epsilon'(T \rightarrow 0)$ is here field dependent. The fact that for $(\text{TMTTF})_2\text{PF}_6$, the SP lattice distortion occurs in the CO—ferroelectric—state may be responsible for the slight increase of the low temperature polarizability in the presence of a field. As lattice effects are involved in both transitions, it appears difficult, however, to predict how both types of order interact and are modified by a magnetic field.

As reported in neutron experiments,¹⁷ we also observe a reduction in the SP transition temperature upon deuteration. However, thermal relaxation effects are observed at microwave frequencies at low temperatures for the D_{12} salt. By deuteration the decrease in internal pressure increases the volume of the anion cavity delimited by the methyl groups. These deuterated groups can thus move more freely and are probably the cause of the anomalous relaxation effects. How-

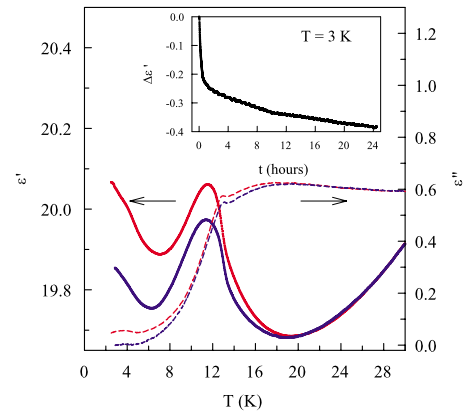


FIG. 5. (Color online) Temperature dependence of the dielectric function near T_{SP} for the D_{12} salt: 2 h (red-gray) and 24 h (blue-black) waiting time at 3 K. The vertical dashed line indicates T_{SP} . Inset: time dependence of $\Delta\epsilon'$ at 3 K.

ever, at the present time we do not have a clear explanation of their impact on both CO and SP orders that coexist in this temperature range. The dielectric function of this salt is shown below 30 K in Fig. 5. The temperature dependence of both parts of ϵ^* is in many respects different from the ones shown in Fig. 3 for the H_{12} salt which is indicative of another mechanism contributing to the dielectric function in this temperature range. However, we can identify features related to the SP transition, that is a sudden slope variation on ϵ' and a sharp peak on ϵ'' at 13.1 K, whose magnetic field variation is similar to the H_{12} case. This contribution is critically dependent on time as evidenced by the two curves appearing in Fig. 5, taken, respectively, 2 and 24 h after the first cooling down to 2 K. In the inset, we present the time dependence of $\Delta\epsilon'$ at $T = 3$ K, just after cooling the sample from 40 K. Two time scales are clearly observed (insert of Fig. 5): a relatively fast one during the first half-hour and a very slow one for which saturation is obtained approximately after 48 h. Similar effects with decreasing amplitude are observed up to 40 K. These thermal relaxation effects related to deuterated methyl groups prevent any analysis of the SP contribution to the dielectric function similar to the one given in Fig. 4 for the hydrogenated samples. These effects also mask the real temperature dependence of the relaxation $\tau(T)$ below 40 K in the CO state (Fig. 2). Nevertheless, our microwave data confirm the decrease of T_{SP} by roughly 30% upon deuteration¹⁷ and its magnetic field dependence $T_{SP}(H)$ could be studied up to 18 T and compared with the hydrogenated salt.

The magnetic field dependence of the SP transition temperature is known to fit a quadratic variation^{36,39} in relatively low fields as predicted theoretically.^{28,38} In the hydrogenated $(\text{TMTTF})_2\text{PF}_6$ salt, NMR and magnetization measurements have indeed revealed some quadratic dependence,²³ but the entire range of low field values for $T_{SP}(H)$ was not available. From our field dependent microwave data, the phase diagram including the D_{12} and H_{12} salts is presented in Fig. 6 and compared to the mean-field prediction (continuous and dash lines) obtained by Cross²⁸

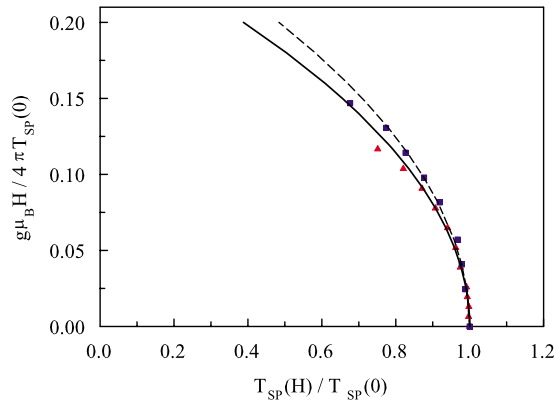


FIG. 6. (Color online) Magnetic field dependence of the reduced SP transition temperature $T_{SP}(H)/T_{SP}(0)$ for the $(\text{TMTTF})_2\text{PF}_6$ salts: red triangles for H_{12} , blue squares for D_{12} ; the continuous and dash lines are the respective fits to Eq. (2).

$$\frac{T_{SP}(H)}{T_{SP}(0)} = \left[1 - c \left(\frac{g\mu_B H}{4\pi T_{SP}(0)} \right)^2 \right], \quad (2)$$

where the g factor is fixed at 2 for $(\text{TMTTF})_2\text{PF}_6$.⁴⁰ For the H_{12} salt, the fit gives $c \approx 15.3$, and $c \approx 12.9$ for the deuterated salt which is relatively close to the predicted value of 14.4,⁴¹ in comparison to other systems such as CuGeO_3 , where pronounced deviations are found.⁴²

IV. CONCLUSION

In $(\text{TMTTF})_2\text{PF}_6$ salts, we found that both the charge ordering and spin-Peierls transitions can be studied from mea-

surements of the microwave dielectric function. In the gigahertz frequency range, the technique is sensitive to short-range polar order, which yields a decrease in the dielectric constant below T_{CO} due to a rapid reduction of these ordered regions and of their relaxation time. The microwave data confirm not only the relaxer character of the CO transition in the hydrogenated salt, but also its stabilization upon deuteration, which increases T_{CO} by 33%. Contrary to systems with no CO ordering, dielectric anomalies are also observed in the SP state for both salts, with a 20% reduction in T_{SP} upon deuteration. The opposite effects of deuteration on T_{SP} and T_{CO} are compatible with an effective negative shift on the pressure axis.

Thermal relaxation effects have been detected in the deuterated salt, which have impeded a complete analysis of the SP ordering. These SP anomalies confirm an indirect coupling between charge, lattice and spin degrees of freedom due to intricate lattice effects in a temperature range where both the SP and CO ground states coexist. A quadratic magnetic field dependence of the SP transition temperature appears to follow the mean-field prediction despite the existence of one-dimensional lattice fluctuations over a wide range of temperature in $(\text{TMTTF})_2\text{PF}_6$.

ACKNOWLEDGMENTS

The authors acknowledge the technical support of Mario Castonguay. This work was supported by grants from the Fonds Québécois de la Recherche sur la Nature et les Technologies (FQRNT) and from the Natural Science and Engineering Research Council of Canada (NSERC).

- ¹C. Bourbonnais and D. Jérôme, in *Physics of Organic Superconductors and Conductors*, Springer Series in Materials Science Vol. 110, edited by A. G. Lebed (Springer, Heidelberg, 2008), p. 357.
- ²S. E. Brown, P. M. Chaikin, and M. J. Naughton, in *Physics of Organic Superconductors and Conductors*, Springer Series in Materials Science Vol. 110, edited by A. G. Lebed (Springer, Heidelberg, 2008), p. 49.
- ³P. Monceau, J.-C. Lasjaunias, K. Biljakovic, and F. Nad, in *Physics of Organic Superconductors and Conductors*, Springer Series in Materials Science Vol. 110, edited by A. G. Lebed (Springer, Heidelberg, 2008), p. 277.
- ⁴C. Coulon, S. Parkin, and R. Laversanne, *Phys. Rev. B* **31**, 3583 (1985).
- ⁵H. H. S. Javadi, R. Laversanne, and A. J. Epstein, *Phys. Rev. B* **37**, 4280 (1988).
- ⁶F. Nad, P. Monceau, and J. M. Fabre, *J. Phys. IV* **09**, PR10 (1999).
- ⁷D. S. Chow, F. Zamborszky, B. Alavi, D. J. Tantillo, A. Baur, C. A. Merlic, and S. E. Brown, *Phys. Rev. Lett.* **85**, 1698 (2000).
- ⁸P. Monceau, F. Ya. Nad, and S. Brazovskii, *Phys. Rev. Lett.* **86**, 4080 (2001).
- ⁹R. Laversanne, C. Coulon, B. Gallois, J. P. Pouget, and R. Moret, *J. Phys. (France) Lett.* **45**, 393 (1984).

- ¹⁰F. Nad, P. Monceau, C. Carcel, and J. M. Fabre, *Phys. Rev. B* **62**, 1753 (2000).
- ¹¹F. Zamborsky, W. Yu, W. Raas, S. Brown, B. Alavic, C. Merlic, A. Baur, S. Lefebvre, and P. Wzietek, *J. Phys. IV* **12**, 139 (2002).
- ¹²S. Fujiyama and T. Nakamura, *J. Phys. Soc. Jpn.* **75**, 014705 (2006).
- ¹³M. Dumm, M. Abaker, and M. Dressel, *J. Phys. IV* **131**, 55 (2005).
- ¹⁴F. Nad and P. Monceau, *J. Phys. Soc. Jpn.* **75**, 051005 (2006).
- ¹⁵J. P. Pouget, R. Moret, R. Comes, K. Bechgaard, J. M. Fabre, and L. Giral, *Mol. Cryst. Liq. Cryst.* **79**, 485 (1982).
- ¹⁶P. Foury-Leylekian, D. Le Bolloc'h, B. Hennion, S. Ravy, A. Moradpour, and J.-P. Pouget, *Phys. Rev. B* **70**, 180405(R) (2004).
- ¹⁷J.-P. Pouget, P. Foury-Leylekian, D. Le Bolloc'h, B. Hennion, S. Ravy, C. Coulon, V. Cardoso, and A. Moradpour, *J. Low Temp. Phys.* **142**, 147 (2006).
- ¹⁸F. Creuzet, C. Bourbonnais, L. G. Caron, D. Jerome, and K. Bechgaard, *Synth. Met.* **19**, 289 (1987).
- ¹⁹M. Dumm, A. Loidl, B. W. Fravel, K. P. Starkey, L. K. Montgomery, and M. Dressel, *Phys. Rev. B* **61**, 511 (2000).
- ²⁰P. Foury-Leylekian, S. Petit, C. Coulon, B. Hennion, A. Moradpour, and J.-P. Pouget, *Physica B* **404**, 537 (2009).

- ²¹P. Wzietek, F. Creuzet, C. Bourbonnais, D. Jérôme, K. Bechgaard, and P. Batail, *J. Phys. I* **3**, 171 (1993).
- ²²F. Zamborszky, W. Yu, W. Raas, S. E. Brown, B. Alavi, C. A. Merlic, and A. Baur, *Phys. Rev. B* **66**, 081103(R) (2002).
- ²³S. E. Brown, W. G. Clark, F. Zamborszky, B. J. Klemme, G. Kriza, B. Alavi, C. Merlic, P. Kuhns, and W. Moulton, *Phys. Rev. Lett.* **80**, 5429 (1998); S. E. Brown, W. G. Clark, B. Alavi, D. Hall, M. J. Naughton, D. J. Tantillo, and C. A. Merlic, *Phys. Rev. B* **60**, 6270 (1999).
- ²⁴C. Bourbonnais and B. Dumoulin, *J. Phys. France* **6**, 1727 (1996).
- ²⁵F. Creuzet, D. Jérôme, and A. Moradpour, *Mol. Cryst. Liq. Cryst.* **119**, 297 (1987).
- ²⁶M. de Souza, P. Foury-Leylekian, A. Moradpour, J.-P. Pouget, and M. Lang, *Phys. Rev. Lett.* **101**, 216403 (2008).
- ²⁷M. de Souza, A. Brühl, J. Müller, P. Foury-Leylekian, A. Moradpour, J.-P. Pouget, and M. Lang, *Physica B* **404**, 494 (2009).
- ²⁸M. C. Cross, *Phys. Rev. B* **20**, 4606 (1979).
- ²⁹F. Wudl, E. Aharon-Shamo, and S. H. Bertz, *J. Org. Chem.* **46**, 4612 (1981).
- ³⁰J. R. Durig, S. E. Hannum, and S. E. Brown, *J. Phys. Chem.* **75**, 1946 (1971).
- ³¹H. Pechamann and F. Dahl, *Chem. Ber.* **23**, 2421 (1890).
- ³²R. M. Magid, B. G. Talley, and S. K. Souther, *J. Org. Chem.* **46**, 824 (1981).
- ³³L. Buravov and J. F. Shchegolev, *Prib. Tekh. Eksp.* **2**, 171 (1971).
- ³⁴C. Coulon, G. Lalet, J.-P. Pouget, P. Foury-Leylekian, A. Moradpour, and J.-M. Fabre, *Phys. Rev. B* **76**, 085126 (2007).
- ³⁵C. S. Jacobsen, D. B. Tanner, and K. Bechgaard, *Phys. Rev. B* **28**, 7019 (1983).
- ³⁶M. Poirier, M. Castonguay, A. Revcolevschi, and G. Dhalenne, *Phys. Rev. B* **52**, 16058 (1995).
- ³⁷S. Allen, J. C. Pieri, C. Bourbonnais, M. Poirier, M. Matos, R. Matos, and R. T. Henriques, *Europhys. Lett.* **32**, 663 (1995).
- ³⁸M. Azzouz and C. Bourbonnais, *Phys. Rev. B* **53**, 5090 (1996).
- ³⁹D. Bloch, J. Voiron, J. C. Bonner, J. W. Bray, I. S. Jacobs, and L. V. Interrante, *Phys. Rev. Lett.* **44**, 294 (1980).
- ⁴⁰C. Coulon, P. Delhaes, S. Flandrois, R. Lagnier, E. Bonjour, and J. M. Fabre, *J. Phys. (Paris)* **43**, 1059 (1982).
- ⁴¹In the theoretical description of strongly anisotropic (quasi-one-dimensional) spin-Peierls systems such as $(\text{TMTTF})_2\text{PF}_6$ [see for example D. J. Scalapino *et al.*, *Phys. Rev. B* **11**, 2042 (1975)], the true transition temperature T_{SP} , close to which critical exponents can reach their non-mean-field values as found in Fig. 4, remains proportional to the mean-field temperature T_{MF} used in Eq. (2). The latter can then approximately describe the field dependence of the true transition.
- ⁴²J. Zeman, G. Martinez, P. H. M. van Loosdrecht, G. Dhalenne, and A. Revcolevschi, *Phys. Rev. Lett.* **83**, 2648 (1999).